

Kinetic Model of Trapped Finite Temperature Binary Condensates

M. J. Edmonds, K. L. Lee, and N. P. Proukakis

Joint Quantum Centre (JQC) Durham-Newcastle, School of Mathematics and Statistics,
Newcastle University, Newcastle upon Tyne NE1 7RU, England, UK

(Dated: December 7, 2024)

We construct a fully self-consistent non-equilibrium theory for the dynamics of two interacting finite-temperature atomic Bose-Einstein condensates. The condensates are described by dissipative Gross-Pitaevskii equations, coupled to quantum Boltzmann equations for the thermal atoms. The density-density interactions between atoms in different components facilitate a number of transport processes of relevance to sympathetic cooling: in particular, identification of an inter-component scattering process associated with collisional "exchange" of condensed and thermal atoms between the components, is found numerically to dominate close to equilibrium, for both realistic miscible and immiscible trapped atomic ^{87}Rb - ^{41}K and ^{87}Rb - ^{85}Rb condensate mixtures.

PACS numbers: 03.75.Mn, 67.85.-d

Introduction. The unprecedented control of trapped neutral cold atom experiments enables the creation and study of degenerate multi-component systems, including Bose-Bose [1], Bose-Fermi [2] and Fermi-Fermi [3, 4] mixtures, and the related problems of spinor gases [5], artificial gauge fields [6] and spin drag [7]. In two-component systems, cooling to quantum degeneracy is typically performed through a combination of evaporative [8] and sympathetic [9] cooling techniques. In the context of bosonic gas mixtures, this leads to condensation either in differing hyperfine states of an atom (^{87}Rb [1, 9–11]), differing isotopes (e.g. ^{87}Rb - ^{85}Rb [12], ^{168}Yb - ^{174}Yb [13]) or differing elements (e.g. ^{87}Rb - ^{41}K [14, 15], ^{87}Rb - ^{133}Cs [16, 17], ^{87}Rb - ^{84}Sr and ^{87}Rb - ^{88}Sr [18], ^{87}Rb - ^{23}Na [19]). Interest in such systems has focused on understanding numerous properties, including their equilibrium profiles [20–24], stability properties [25, 26], excitation spectrum [21, 27], vortices [28] and solitary-wave structures [29], as well as dissipative [30] and quenched dynamics [31]; the above depend critically on the relative effective inter-atomic interactions within and between the species, which determine whether the emerging condensates overlap spatially or phase-separate [20, 21].

Due to its intrinsic complexity, the description of bosonic components in mixtures are typically either focused on the low temperature (Gross-Pitaevskii) [32], or high-temperature (Boltzmann) limit [33–35], or on treating the condensate in contact with a static heat bath [36–38]. Recent alternative approaches are based on either classical field methods (which ignore the dynamics of the high-lying thermal modes [31, 39]), or on number-conserving methods (which explicitly include only the back-action of the thermal cloud on the condensate [40, 41]). Moreover, although related self-consistent kinetic models have been analytically derived in the context of spinor gases [42, 43], there has been to date no critical assessment of the role of all relevant arising collisional processes at finite temperatures.

In this work we present a unified self-consistent model for the study of partly-condensed bosonic mixtures in the presence of dynamical condensates and thermal clouds

which includes all arising collisional processes, as shown schematically in Fig. 1. By performing numerical calculations, we explicitly classify the relative importance of all depicted collisional terms near equilibrium for experimentally-accessible mixtures both in the miscible, and immiscible regimes; in particular, our analysis reveals an additional means to exchange energy between two condensates, which could bring new insight into the late evolutionary stages of sympathetic cooling.

Our approach is a generalization of the "Zaremba-Nikuni-Griffin" (ZNG) kinetic model [44–47] which, in the context of single-component condensates, has proven extremely useful in describing collective modes [48], condensate growth [49], dynamics of macroscopic excitations [50] and surface evaporative cooling [51]. In brief, this approach is based on the decomposition of the Bose field operator into a symmetry-breaking part and its fluctuations, and a separation of timescales argument (see also [52–55]): in undertaking the analysis, we explicitly separate slowly-evolving variables for the condensate and thermal clouds, whose non-vanishing mean values are defined by appropriate dynamical equations, from those evolving on the more rapid collisional timescales. A care-

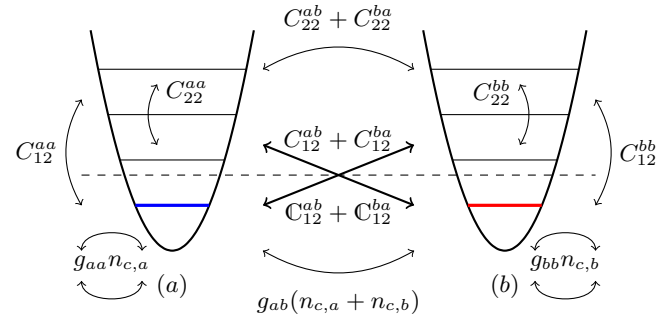


FIG. 1: (Color online) Schematic representation of our collisional model. The two trapped condensates are denoted (a) (left) and (b) (right). Arrows indicate the various mean field and collisional transport processes occurring within and between the condensates and non-condensates of the different component.

ful self-consistent perturbative analysis of such terms in the context of an appropriate perturbing Hamiltonian (details to appear elsewhere) reveals collisional processes, not accounted for in Refs. [42, 43], which we quantify for the first time here.

Coupled Kinetic Theory. The Hamiltonian describing the interacting two-component system can be written in second-quantized form as

$$\hat{H} = \sum_{j=a}^b \int d\mathbf{r} \hat{\Psi}_j^\dagger(\mathbf{r}) \left(-\frac{\hbar^2}{2m_j} \nabla^2 + V_j(\mathbf{r}) \right) \hat{\Psi}_j(\mathbf{r}) + \frac{1}{2} \sum_{k,j=a}^b g_{kj} \int d\mathbf{r} \hat{\Psi}_j^\dagger(\mathbf{r}) \hat{\Psi}_k^\dagger(\mathbf{r}) \hat{\Psi}_k(\mathbf{r}) \hat{\Psi}_j(\mathbf{r}), \quad (1)$$

where $\hat{\Psi}_j(\mathbf{r})$ is the annihilation operator for a species- j atom. The effective interaction strength for low energy s -wave collisions is defined as $g_{kj} = 2\pi\hbar^2 a_{kj}/m_{kj}$, where a_{kj} is the scattering length between atoms in component j and k , $m_{kj}^{-1} = m_k^{-1} + m_j^{-1}$ defines the reduced mass, with m_j the mass of a boson in component j ; finally the trapping potential for component j is given by $V_j(\mathbf{r})$.

To separate the condensate components, ϕ_j , from non-condensed parts of the system, we perform the Beliaev decomposition $\hat{\Psi}_j = \phi_j + \hat{\delta}_j$. The condensate evolution equations are thus obtained from the Heisenberg equations of motion for $\hat{\Psi}_j$ upon taking averages with respect to a broken-symmetry non-equilibrium ensemble. The corresponding non-condensed degrees of freedom are described using a Wigner distribution, whose equation of motion is extracted via the non-equilibrium density matrix of the system.

To facilitate a "two-fluid" description of each component as in the usual ZNG theory [44–46], we identify the condensate fields ϕ_j (corresponding condensate densities $n_{c,j} = |\phi_j|^2$), and *diagonal* non-condensate densities $\tilde{n}_j = \langle \hat{\delta}_j^\dagger \hat{\delta}_j \rangle$ as the only relevant *slowly-varying* quantities of interest; *off-diagonal* density elements $\langle \hat{\delta}_j^\dagger \hat{\delta}_k \rangle$ and pair/triplet anomalous averages $\langle \hat{\delta}_k \hat{\delta}_j \rangle$, $\langle \hat{\delta}_k^\dagger \hat{\delta}_k \hat{\delta}_j \rangle$ are treated perturbatively via adiabatic elimination [52, 53], only maintaining energy-conserving contributions in our perturbative analysis (hence maintaining no additional pair anomalous average contribution $\langle \hat{\delta}_k \hat{\delta}_j \rangle$ [56]).

The equation of motion for component j takes the form

$$i\hbar \frac{\partial \phi_j}{\partial t} = \left[-\frac{\hbar^2}{2m_j} \nabla^2 + V_j(\mathbf{r}) + g_{jj}(n_{c,j} + 2\tilde{n}_j) + g_{kj}(n_{c,k} + \tilde{n}_k) - i(R^{jj} + R^{kj}) - i\mathbb{R}^{kj} \right] \phi_j, \quad (2)$$

with $j, k \in \{a, b\}$. In addition to the usual mean-field contributions, Eq. (2) introduces the dissipative kinetic contributions R^{jj} , R^{kj} and \mathbb{R}^{kj} . The first of these, $R^{jj} = -ig_{jj}\langle \hat{\delta}_j^\dagger \hat{\delta}_j \hat{\delta}_j \rangle/\phi_j$, describes the intra-component scattering of condensate and non-condensate particles forming the basis of single-component ZNG theory [44, 45],

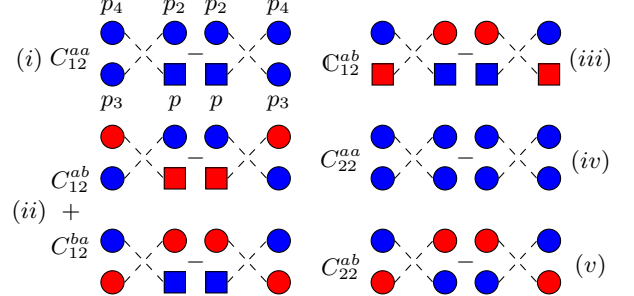


FIG. 2: (Color online) Each diagram represents a kinetic energy and momentum conserving collision between atoms. Squares and circles represent condensate and thermal atoms respectively. Component a particles are blue, while b are red. Diagrams for the b component are obtained by interchanging the two colors in each square and circle.

while the second, $R^{kj} = -ig_{kj}\langle \hat{\delta}_k^\dagger \hat{\delta}_k \hat{\delta}_j \rangle/\phi_j$, describes the inter-component scattering of atoms. The final term, $\mathbb{R}^{kj} = -ig_{kj}\langle \hat{\delta}_k^\dagger \hat{\delta}_j \rangle/\phi_j/\phi_k$, is qualitatively different from the other two, as explained below. The calculation of such kinetic contributions appearing in Eq. (2) requires a non-equilibrium average which is accomplished using the general density matrix of the multi-component system. (see, e.g. Refs. [42–45]). In order to construct a closed set of dynamical equations for the coupled time evolution of the condensate and non-condensate fractions, the multi-component single-particle Wigner distribution is introduced in the form $f^{kj}(\mathbf{p}, \mathbf{r}, t) = \int d\mathbf{r}' e^{i\mathbf{p} \cdot \mathbf{r}'/\hbar} \langle \hat{\delta}_j^\dagger(\mathbf{r} + \mathbf{r}'/2, t) \hat{\delta}_k(\mathbf{r} - \mathbf{r}'/2, t) \rangle$. In this work, we restrict our analysis to the diagonal terms of the Wigner operator, i.e. $f^{jj}(\mathbf{p}, \mathbf{r}, t) \equiv f^j(\mathbf{p}, \mathbf{r}, t)$ an approximation that is valid in the absence of coherent couplings between states. (see Ref. [42] for inclusion of off-diagonal terms in the Wigner operator in the context of spinor condensates.) The kinetic equation for component j is

$$\frac{\partial}{\partial t} f^j + \frac{1}{m_j} \mathbf{p} \cdot \nabla_{\mathbf{r}} f^j - \nabla_{\mathbf{p}} f^j \cdot \nabla_{\mathbf{r}} U_{\text{eff}}^j = (C_{12}^{jj} + C_{12}^{kj}) + \mathbb{C}_{12}^{kj} + (C_{22}^{jj} + C_{22}^{kj}). \quad (3)$$

The effective (Hartree-Fock) potential that thermal atoms in component j feel is given by $U_{\text{eff}}^j = V_j(\mathbf{r}) + 2g_{jj}[n_{c,j} + \tilde{n}_j] + g_{kj}[n_{c,k} + \tilde{n}_k]$, and the non-condensate density of component j can be computed by integrating over all momentum of the distribution function $\tilde{n}_j(\mathbf{r}, t) = \int d\mathbf{p}/(2\pi\hbar)^3 f^j(\mathbf{p}, \mathbf{r}, t)$. The dissipative terms appearing in Eq. (2) are related to the collision integrals by the relationships $-2n_{c,j}R^{kj}/\hbar = \int d\mathbf{p}/(2\pi\hbar)^3 C_{12}^{kj}$ and $-2n_{c,j}\mathbb{R}^{kj}/\hbar = \int d\mathbf{p}/(2\pi\hbar)^3 \mathbb{C}_{12}^{kj}$. The various collisional contributions to the kinetic scattering of particles for the a component are summarised in Fig. 2. The first three diagrams, labelled (i)-(iii) concern collision integrals describing the scattering of condensed and non-condensate particles, while the diagrams labelled (iv) and (v) show scattering amongst non-condensed atoms.

The collision integral C_{12}^{kj} (encapsulating C_{12}^{jj}) appearing in Eq. (3) is defined by

$$C_{12}^{kj} = (1 + \delta_{kj}) \frac{g_{kj}^2}{(2\pi)^2 \hbar^4} \int d\mathbf{p}_2 \int d\mathbf{p}_3 \int d\mathbf{p}_4$$

$$\times \left\{ n_{c,k} \delta(\mathbf{p}_c^k + \mathbf{p}_2 - \mathbf{p}_3 - \mathbf{p}_4) \delta(\varepsilon_c^k + \varepsilon_{p_2}^j - \varepsilon_{p_3}^j - \varepsilon_{p_4}^k) \right.$$

$$\times [(f_2^j + 1)f_3^j f_4^k - f_2^j(f_3^j + 1)(f_4^k + 1)][\delta(\mathbf{p} - \mathbf{p}_2) - \delta(\mathbf{p} - \mathbf{p}_3)]$$

$$- n_{c,j} \delta(\mathbf{p}_c^j + \mathbf{p}_2 - \mathbf{p}_3 - \mathbf{p}_4) \delta(\varepsilon_c^j + \varepsilon_{p_2}^k - \varepsilon_{p_3}^k - \varepsilon_{p_4}^j)$$

$$\left. [(f_2^k + 1)f_3^k f_4^j - f_2^k(f_3^k + 1)(f_4^j + 1)]\delta(\mathbf{p} - \mathbf{p}_4) \right\}, \quad (4)$$

where $f_\mu^k \equiv f^k(\mathbf{p}_\mu, \mathbf{r}, t)$. This collision integral describes the scattering of a condensate atom and a non-condensate atom into thermal states, and its inverse process (see Fig. 2(i)-(ii)), with the Kronecker delta δ_{kj} accounting for enhanced scattering of atoms within the same species (C_{12}^{jj} subcase). In Eq. (4), we define the Hartree-Fock energy as $\varepsilon_p^j = p^2/2m_j + U_{\text{eff}}^j$, while the condensate energy is given by $\varepsilon_c^j = \mu_c^j + \frac{1}{2}m_j v_{c,j}^2$. The condensate momentum for component j is then defined by $\mathbf{p}_c^j = m_j \mathbf{v}_{c,j}$.

Unlike all other collision integrals in ZNG theory which are generated from triplet anomalous averages [45, 52], the collision integral C_{12}^{kj} of Eq. (3) is instead defined from the average of an off-diagonal pair of fluctuation operators, $\langle \hat{\delta}_j^\dagger \hat{\delta}_k \rangle$ ($j \neq k$), and is written as

$$C_{12}^{kj} = \frac{2\pi g_{kj}^2}{\hbar} n_{c,k} n_{c,j} \int d\mathbf{p}_1 \int d\mathbf{p}_2$$

$$\times \delta(\mathbf{p}_c^j + \mathbf{p}_1 - \mathbf{p}_c^k - \mathbf{p}_2) \delta(\varepsilon_c^j + \varepsilon_{p_1}^k - \varepsilon_c^k - \varepsilon_{p_2}^j)$$

$$\times [(f_2^j + 1)f_1^k - f_2^j(f_1^k + 1)]\delta(\mathbf{p} - \mathbf{p}_2). \quad (5)$$

This expression is qualitatively different to the collision integral of Eq. (4), as it describes a process whereby one condensate and one non-condensate atom from different components scatter into a thermal and condensed state respectively, as depicted in Fig. 2(iii). Such a process can only appear in a physical system with a minimum of two internal degrees of freedom. This process is expected to become important in the latter stages of sympathetic cooling, when both components exhibit (partial) condensation.

The final collision process to be described for the multi-component system is the scattering between non-condensate atoms of the same or differing species. The general form of the collision integral for these scattering events (both for $j = k$ and $j \neq k$) is

$$C_{22}^{kj} = (1 + \delta_{kj}) \frac{g_{kj}^2}{(2\pi)^5 \hbar^7} \int d\mathbf{p}_2 \int d\mathbf{p}_3 \int d\mathbf{p}_4$$

$$\times \delta(\mathbf{p} + \mathbf{p}_2 - \mathbf{p}_3 - \mathbf{p}_4) \delta(\varepsilon_p^j + \varepsilon_{p_2}^k - \varepsilon_{p_3}^k - \varepsilon_{p_4}^j)$$

$$[(f_2^j + 1)(f_{p_2}^k + 1)f_{p_3}^k f_{p_4}^j - f^j f_{p_2}^k(f_{p_3}^k + 1)(f_{p_4}^j + 1)]. \quad (6)$$

Numerical Results. To gain insight into the relative importance of the scattering processes, we numerically

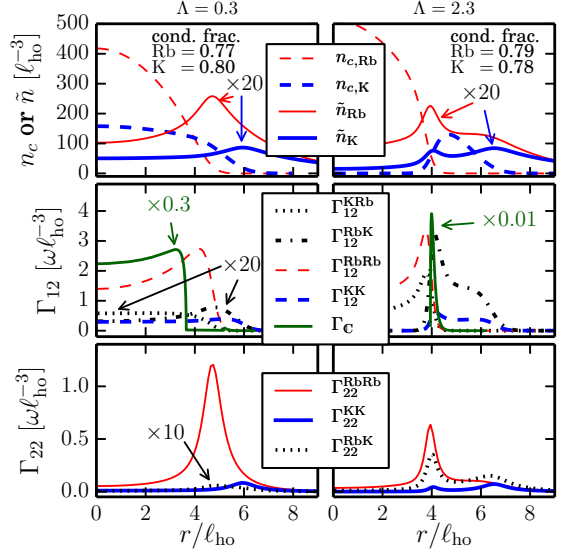


FIG. 3: (Color online) Miscible (left) and immiscible (right) ^{87}Rb - ^{41}K mixture in isotropic harmonic trap (trap frequency $\omega = 2\pi \times 20\text{Hz}$) at temperature 21nK with scattering lengths $a_{\text{Rb87}} = 99a_0$, $a_{\text{K}} = 60a_0$, $a_{\text{Rb-K}} = 20a_0$ (miscible) or $163a_0$ (immiscible) [14, 15]; each species has a total of $N = 10^5$ atoms. The non-interacting single-component critical temperature is $T_c \approx 0.94\hbar\omega N^{1/3}/k_B \approx 42\text{nK}$. (Top) Condensate and thermal densities. (Middle) Spatially-resolved collision rates between condensate and thermal atoms. (Bottom) Spatially-resolved collision rates between thermal atoms.

compute the collision rates at various temperatures for the experimentally-relevant cases of equilibrium ^{87}Rb - ^{41}K and ^{87}Rb - ^{85}Rb mixtures for a total atom number $N_j = 10^5$ in each component, confined in an isotropic harmonic trap of frequency $\omega = 2\pi \times 20\text{Hz}$. These specific mixtures have been chosen here as their tunable scattering lengths [12, 14, 15] enable the probing of both miscible $\Lambda = g_{12}/\sqrt{g_{11}g_{22}} < 1$ and immiscible ($\Lambda > 1$) regimes. By re-expressing $C_{12}^{kj} = C_{12}^{kj,\text{out}} - C_{12}^{kj,\text{in}}$ (and analogously for C_{12}^{kj} and C_{22}^{kj}), we explicitly identify "in" and "out" scattering rates, which are equal at equilibrium. Following Ref. [44, 47], we thus define collisional rates $\Gamma_{12(22)}^{kj} = \int d\mathbf{p}/(2\pi\hbar)^3 C_{12(22)}^{kj,\text{out}}$, giving the number of atoms leaving a phase-space volume $dr d\mathbf{p}/\hbar^3$ per unit time as a result of collisions, for a perturbation from equilibrium. By transforming to the centre of mass frames, the collision rates can be written as $\Gamma_{12}^{kj} = \int \frac{d\mathbf{p}_2}{(2\pi\hbar)^3} f_2^k n_{c,j} \sigma_{kj} v_r \int \frac{d\Omega}{4\pi} (f_3^k + 1)(f_4^j + 1)$, where v_r is the relative velocity and $\sigma_{kj} = (1 + \delta_{kj})4\pi a_{kj}^2$ the cross-section. The collision rates between non-condensate atoms is $\Gamma_{22}^{kj} = \int \frac{d\mathbf{p}_1}{(2\pi\hbar)^3} f_1^j \int \frac{d\mathbf{p}_2}{(2\pi\hbar)^3} f_2^k \int \frac{d\Omega}{4\pi} \sigma_{kj} |\mathbf{v}_1 - \mathbf{v}_2| (f_3^k + 1)(f_4^j + 1)$, while the scattering rate associated with C_{12}^{kj} type collisions, defined by $\Gamma_{\text{C}}^{kj} = \int d\mathbf{p}/(2\pi\hbar)^3 C_{12}^{kj,\text{out}}$ takes the form

$$\Gamma_{\text{C}}^{kj} = \sigma_{kj} \left(\frac{\mathcal{M}_{kj}}{m_{kj}} \right)^2 n_{c,k} n_{c,j} \tilde{v}_r \int \frac{d\Omega}{4\pi} f_2^j (f_1^k + 1), \quad (7)$$

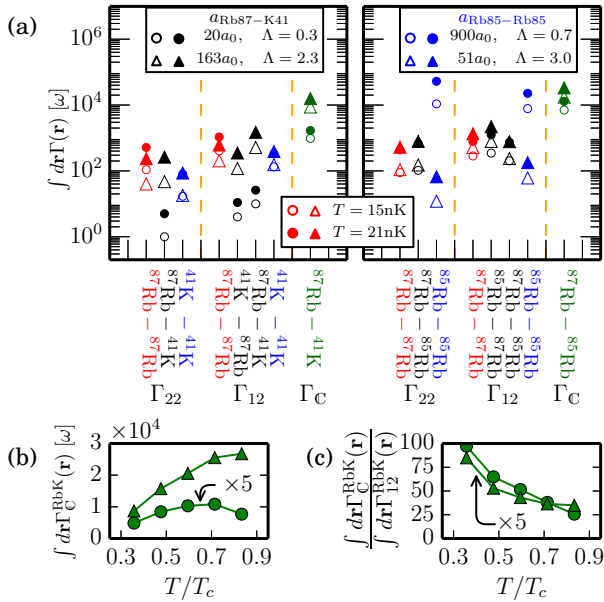


FIG. 4: (Color online) (a) Comparison of integrated collision rates among the various processes at different temperatures and miscibilities for (left) $^{87}\text{Rb}-^{41}\text{K}$ ($a_{\text{Rb}} = 99a_0$, $a_{\text{K}} = 60a_0$) and (right) $^{87}\text{Rb}-^{85}\text{Rb}$ ($a_{\text{Rb87-Rb85}} = 99a_0$, $a_{\text{Rb87-Rb85}} = 213a_0$ [12]) mixtures; other parameters as in Fig. 3. (Bottom) Corresponding temperature dependence for $^{87}\text{Rb}-^{41}\text{K}$ mixtures of (b) integrated collision rates of $\text{C}_{12}^{\text{RbK}}$ and (c) ratio of integrated collision rates of $\text{C}_{12}^{\text{RbK}}$ to that of $\text{C}_{12}^{\text{RbRb}}$.

with \tilde{v}_r the relative velocity and $\mathcal{M}_{kj}^{-1} = m_k^{-1} - m_j^{-1}$. Figure 3 shows the equilibrium condensate/thermal density profiles (top panels) and collision rates (middle/bottom panels) for a mixture of ^{87}Rb and ^{41}K at a temperature of $T = 21\text{nK}$, when condensate fractions $\approx 80\%$, for both miscible ($\Lambda = 0.3$, left column) and immiscible ($\Lambda = 2.1$, right column) cases. The two condensates depicted by the dashed lines mix (top panel, left) or phase-separate (top panel, right) with thermal clouds (solid lines) displaying peaks at the condensate edges, thus also leading to a mean-field-induced double-peaked thermal structure. The spatially-resolved collisional rates between condensate and non-condensate (middle panels) reveal peaks close to the condensate edges, which become more pronounced for immiscible condensates. In particular, $\text{C}_{12}^{\text{RbK}}$ collisional rates feature large localized peaks in regions where both components exhibit an appreciable condensate, which can locally dominate all other collisional processes in the centre of the immiscibility region. Collision rates between non-condensate atoms (bottom panels) are found to closely follow the shape of the non-condensate profiles, with the inter-species rates, Γ_{22}^{RbK} (black-dotted line), affected by both thermal cloud distributions.

The cumulative effect of such collisional processes is

best characterized through the integrated collision rates, obtained from integrating Γ_{22}^{kj} , Γ_{12}^{kj} and Γ_{C}^{kj} over the volume of the cloud, shown in Fig. 4. Fig. 4(a) shows both $^{87}\text{Rb}-^{41}\text{K}$ (left panels), and $^{87}\text{Rb}-^{85}\text{Rb}$ mixtures (right panels), in their experimentally-accessible miscibility (circles) and immiscibility (triangles) regimes for the $T = 21\text{nK}$ case of Fig. 3 (filled symbols) and for $T = 15\text{nK}$ (open symbols). We find a number of key results: (i) the novel C_{12}^{kj} collisions (green symbols) are at least as large as the other collisional terms in all cases; (ii) increasing the temperature (hollow to filled symbols) in the presence of an appreciable condensate fraction, enhances all collisional rates involving thermal atoms, including C_{12}^{kj} and C_{22}^{kj} , despite the simultaneous reduction in condensate fraction; (iii) collisional rates are largely sensitive to effective interaction strength g_{kj} (through g_{kj}^2 prefactors), which can be controlled through Feshbach resonances: an increase in the inter-species scattering length $a_{\text{Rb87-K41}}$ [14, 15] (left image) increases the relative importance of all $^{87}\text{Rb}-^{41}\text{K}$ thermal-thermal, or condensate-thermal collisional terms (black/green points). Likewise, an increase in one of the intra-component scattering lengths, namely the tunable $a_{\text{Rb85-Rb85}}$ [12] (right), mostly affects the $^{85}\text{Rb}-^{85}\text{Rb}$ (blue) collisional terms. To illustrate the importance of the novel C_{12}^{kj} collisional process, Fig. 4(b)-(c) shows the temperature dependence of their integrated rates (b), and their ratios to the corresponding integrated Γ_{12}^{RbK} rates (c) for $^{87}\text{Rb}-^{41}\text{K}$ mixtures. The large values of the ratios (in the range 5-100) at all probed temperatures ($0.3 < T/T_c < 0.9$) and their rapid increase with decreasing temperature for the selected configurations demonstrate the crucial role that the C_{12}^{kj} collisional terms may play during various sympathetic cooling stages.

Conclusions. We have presented a fully self-consistent system of coupled kinetic equations for the evolution of two-component condensates in the presence of dynamical thermal clouds, incorporating all collisional processes in the absence of critical fluctuations. Numerical calculations of the relative importance of the arising collisional processes, identified a novel "cross-condensate-exchange" term, potentially crucial in the equilibrating stages of sympathetic cooling. Our work, which is generalizable to multi-component Bose gases and Bose-Fermi mixtures, sets the scene for future dynamical studies of sympathetic cooling and multi-component condensate formation.

Acknowledgements. We acknowledge stimulating discussions with S.L. Cornish, S.A. Gardiner, P. Mason, E. Zaremba and M. Edwards. M.J.E acknowledges support from an EPSRC Doctoral Prize Fellowship, K.L.L and N.P.P acknowledge support from EPSRC grant EP/K03250X/1.

[1] D. S. Hall, M. R. Matthews, J. R. Ensher, C. E. Wieman, and E. A. Cornell, *Phys. Rev. Lett.* **81**, 1539 (1998).

[2] Z. Hadzibabic, C. A. Stan, C. A. Dieckmann, S. Gupta,

M. W. Zwierlein, A. Görlitz, and W. Ketterle, *Phys. Rev. Lett.* **88**, 160401 (2002).

[3] B. DeMarco and D. S. Jin, *Science* **285**, 1703 (1999).

[4] M. Taglieber, A.-C. Voigt, T. Aoki, T. W. Hänsch, and K. Dieckmann, *Phys. Rev. Lett.* **100**, 010401 (2008).

[5] D. M. Stamper-Kurn and M. Ueda, *Rev. Mod. Phys.* **85**, 1191 (2013).

[6] J. Dalibard, F. Gerbier, G. Juzeliūnas, and P. Öhberg, *Rev. Mod. Phys.* **83**, 1523 (2011).

[7] H. J. van Driel, R. A. Duine, and H. T. C. Stoof, *Phys. Rev. Lett.* **105**, 155301 (2010); S.B. Koller, A. Groot, P.C. Bons, R.A. Duine, H.T.C. Stoof, P. van der Straten, arXiv:1204.6143.

[8] W. Ketterle and N. J. Van Druten, *Adv. Atom. Mol. Opt. Phys.* **37**, 181 (1996).

[9] C. J. Myatt, E. A. Burt, R. W. Ghrist, E. A. Cornell, and C. E. Wieman, *Phys. Rev. Lett.* **78**, 586 (1997).

[10] P. Maddaloni, M. Modugno, C. Fort, F. Minardi, and M. Inguscio, *Phys. Rev. Lett.* **85**, 2413 (2000).

[11] K. M. Mertes, J. W. Merrill, R. Carretero-González, D. J. Frantzeskakis, P. G. Kevrekidis, and D. S. Hall, *Phys. Rev. Lett.* **99**, 190402 (2007).

[12] S. B. Papp, J. M. Pino, and C. E. Wieman, *Phys. Rev. Lett.* **101**, 040402 (2008).

[13] S. Sugawa, R. Yamazaki, S. Taie, and Y. Takahashi, *Phys. Rev. A* **84**, 011610(R) (2011).

[14] G. Modugno, M. Modugno, F. Riboli, G. Roati, and M. Inguscio, *Phys. Rev. Lett.* **89**, 190404 (2002).

[15] G. Thalhammer, G. Barontini, L. De Sarlo, J. Catani, F. Minardi, and M. Inguscio, *Phys. Rev. Lett.* **100**, 210402 (2008).

[16] D. J. McCarron, H. W. Cho, D. L. Jenkin, M. P. Köppinger, and S. L. Cornish, *Phys. Rev. A* **84**, 011603(R) (2011).

[17] A. D. Lercher, T. Takekoshi, M. Debatin, B. Schuster, R. Rameshan, F. Ferlaino, R. Grimm, H. -C. Nägerl, *Eur. Phys. J. D* **65**, 3 (2011).

[18] B. Pasquiou, A. Bayerle, S. M. Tzanova, S. Stellmer, J. Szczepkowski, M. Parigger, R. Grimm, and F. Schreck, *Phys. Rev. A* **88**, 023601 (2013).

[19] D. Xiong, X. Li, F. Wang, D. Wang, e-print arXiv:1305.7091

[20] T.-L. Ho and V. B. Shenoy, *Phys. Rev. Lett.* **77**, 3276 (1996).

[21] H. Pu and N. P. Bigelow, *Phys. Rev. Lett.* **80**, 1130 (1998); **80**, 1134 (1998).

[22] P. Öhberg and S. Stenholm, *Phys. Rev. A* **57**, 1272 (1998).

[23] M. Trippenbach, K. Góral, K. Rzążewski, B. Malomed and Y. B. Band, *J. Phys. B: At. Mol. Opt. Phys.* **33**, 4017 (2000).

[24] R. W. Pattinson, T. P. Billam, S. A. Gardiner, D. J. McCarron, H. W. Cho, S. L. Cornish, N. G. Parker, and N. P. Proukakis, *Phys. Rev. A* **87**, 013625 (2013).

[25] P. Öhberg, *Phys. Rev. A* **59**, 634 (1999).

[26] N. P. Robins, W. Zhang, E. A. Ostrovskaya, and Y. S. Kivshar, *Phys. Rev. A* **64**, 021601 (2001).

[27] C.-H. Zhang and H. A. Fertig, *Phys. Rev. A* **75**, 013601 (2007).

[28] E. J. Mueller and T.-L. Ho, *Phys. Rev. Lett.* **88**, 180403 (2002).

[29] N. G. Berloff *Phys. Rev. Lett.* **94**, 120401 (2005).

[30] R. W. Pattinson, N. G. Parker, and N. P. Proukakis, *J. Phys.: Conf. Ser.* **497**, 012029 (2014).

[31] I.-K. Liu, R. W. Pattinson, T. P. Billam, S. A. Gardiner, S. L. Cornish, T.-M. Huang, W.-W. Lin, S.-C. Gou, N. G. Parker and N. P. Proukakis, arXiv:1408.0891

[32] C. J. Pethick and H. Smith, *Bose-Einstein Condensation in Dilute Gases* (Cambridge University Press, Cambridge, 2002).

[33] G. Delannoy, S. G. Murdoch, V. Boyer, V. Josse, P. Bouyer, and A. Aspect, *Phys. Rev. A* **63**, 051602(R) (2001).

[34] A. Mosk, S. Kraft, M. Mudrich, K. Singer, W. Wohlleben, R. Grimm, M. Weidemüller, *Appl. Phys. B* **73**, 791 (2001).

[35] M. Anderlini, D. Ciampini, D. Cossart, E. Courtade, M. Cristiani, C. Sias, O. Morsch, and E. Arimondo, *Phys. Rev. A* **72**, 033408 (2005).

[36] M. Lewenstein, J. I. Cirac, and P. Zoller, *Phys. Rev. A* **51**, 4617 (1995).

[37] E. Timmermans and R. Côté, *Phys. Rev. Lett.* **80**, 3419 (1998).

[38] T. Papenbrock, A. N. Salgueiro, and H. A. Weidenmüller, *Phys. Rev. A* **66**, 025603 (2002).

[39] A. S. Bradley and P. B. Blakie, *Phys. Rev. A* **90**, 023631 (2014).

[40] T. P. Billam, P. Mason, and S. A. Gardiner, *Phys. Rev. A* **87**, 033628 (2013).

[41] P. Mason and S. A. Gardiner, *Phys. Rev. A* **89**, 043617 (2014).

[42] T. Nikuni and J. E. Williams, *J. Low Temp. Phys.* **133**, 323 (2003).

[43] Y. Endo and T. Nikuni, *J. Low Temp. Phys.* **163**, 92 (2011).

[44] A. Griffin, T. Nikuni, and E. Zaremba, *Bose-Condensed Gases at Finite Temperatures* (Cambridge University Press, Cambridge, 2009).

[45] E. Zaremba, T. Nikuni, and A. Griffin, *J. Low. Temp. Phys.* **116**, 277 (1999).

[46] T. Nikuni, E. Zaremba, and A. Griffin, *Phys. Rev. Lett.* **83**, 10 (1999).

[47] B. Jackson and E. Zaremba, *Phys. Rev. A* **66**, 033606 (2002).

[48] B. Jackson and E. Zaremba, *Phys. Rev. Lett.* **87** 100404 (2001); **89** 150402 (2002); *New J. Phys.* **5** 88 (2003).

[49] M. J. Bijlsma, E. Zaremba, and H. T. C. Stoof, *Phys. Rev. A* **62**, 063609 (2000).

[50] B. Jackson, N. P. Proukakis, and C. F. Barenghi, *Phys. Rev. A* **75**, 051601(R) (2007).

[51] J. Märkle, A. J. Allen, P. Federsel, B. Jetter, A. Günther, J. Fortagh, N. P. Proukakis, and T. E. Judd, *Phys. Rev. A* **90**, 023614 (2014).

[52] N. P. Proukakis, K. Burnett, and H. T. C. Stoof, *Phys. Rev. A* **57**, 1230 (1998).

[53] N. P. Proukakis and B. Jackson, *J. Phys. B: At. Mol. Opt. Phys.* **41**, 203002 (2008).

[54] R. Walser, J. Williams, J. Cooper, and M. Holland, *Phys. Rev. A* **59**, 3878 (1999).

[55] J. Wachter, R. Walser, J. Cooper, and M. Holland, *Phys. Rev. A* **64** 053612 (2001).

[56] A. Griffin *Phys. Rev. B* **53**, 9341 (1996).